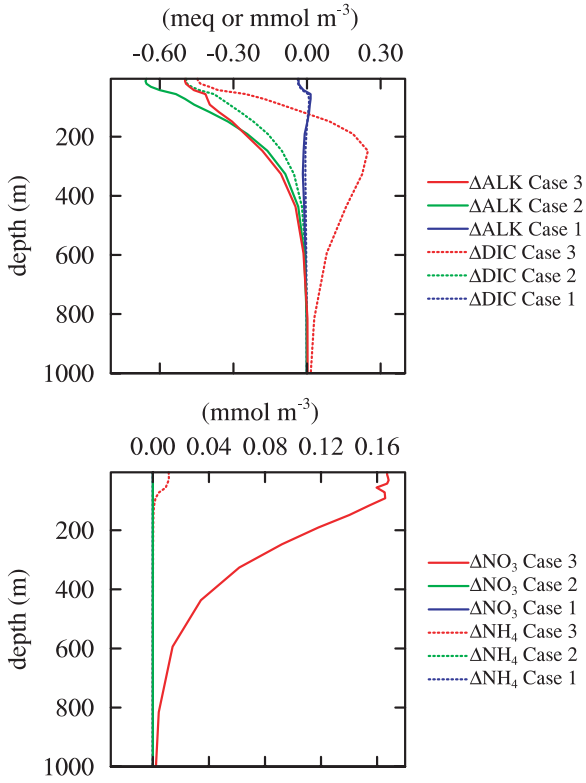

Fig. 2. Perturbations to simulated global vertical profiles due to 10 years of anthropogenic atmospheric nitrogen and sulfur deposition. (*Upper*) Alkalinity (solid lines) and DIC (dashed lines). (*Lower*) NO_3^- (solid lines) and NH_4^+ (dashed lines). Case 1 is forced with alkalinity flux from Fig. 1, case 2 with the potential alkalinity flux (assuming complete nitrification), and case 3 with alkalinity and nitrogen fluxes allowing for biological feedbacks.

experiments. Case 1 simulates direct alkalinity perturbations with no nutrient fertilization; *f*Alk alters surface [Alk]. Case 2 is similar to case 1, except assuming complete nitrification of $fNH_4^+ + fNH_3$; $fAlk_{nitrif}$ alters surface [Alk]. Case 3 incorporates explicit nitrogen cycle perturbations and allows for nutrient fertilization; *f*Alk alters surface [Alk], fNO_3^- alters surface $[NO_3^-]$, and $fNH_4^+ + fNH_3$ alters surface $[NH_4^+]$. All cases and a control (no atmospheric nitrogen and sulfur deposition) are integrated from 1990 to 2000, with repeat annual physics and increasing anthropogenic atmospheric CO_2 based on observations.

The direct effects of anthropogenic nitrogen and sulfur deposition in case 1 are small, in global integral, because alkalinity reductions from fNO_3^- and $fSO_4^- + fSO_2$ are nearly balanced by increases from $fNH_4^+ + fNH_3$ (Fig. 2). In case 2, with complete nitrification, we find a more clear reduction in surface water pH, [Alk], and [DIC] relative to the control simulation (Figs. 2 and 3). The lower surface water [DIC] arises because the negative [Alk] perturbations raise $[pCO_2]$ and drive a perturbation efflux of CO_2 into the atmosphere, counter to the anthropogenic CO_2 flux. The negative Δ[DIC] perturbations are comparable, although slightly smaller than Δ[Alk] in an absolute sense, so that pH still declines but with significantly smaller amplitude than would occur from the original Δ[Alk] perturbation alone. The largest surface water anomalies are found in coastal regions surrounding the emission areas, with trends $\Delta pH/\Delta t$ of -0.02 to -0.12×10^{-3} pH units·y^{-1}, $\Delta[Alk]/\Delta t$ of -0.05 to -0.40 meq·m^{-3}·y^{-1}, and $\Delta[DIC]/\Delta t$ of -0.05 to -0.30 mmol·m^{-3}·y^{-1}. For comparison, the temporal trends in the anthropogenic CO_2 control simulation are $\Delta pH/\Delta t$ of -0.8 to -1.8×10^{-3} pH units·y^{-1} and $\Delta[DIC]/\Delta t$ of $+0.4$ mmol·m^{-3}·y^{-1} near the poles to $+1.2$ mmol·m^{-3}·y^{-1} in the subtropics.

Biological feedbacks depend on three factors: (*i*) the extent to which nitrification transforms excess NH_4^+ into NO_3^-; (*ii*) vertical redistribution of the excess nitrogen by means of biological nitrogen uptake in the surface, particle sinking, and subsurface remineralization; and (*iii*) biological drawdown of surface [DIC] from eutrophication. The effect of primary production on alkalinity depends on the source of nitrogen (31, 32). NO_3^--supported growth produces alkalinity (+1:1 eq/mol), and NH_4^+-supported growth removes alkalinity (−1:1 eq/mol):

$$106CO_2 \quad 16NO_3^- \quad 138H_2O \rightarrow \text{organics} \quad 16OH^- \quad 138O_2 \qquad [10]$$

$$106CO_2 \quad 16NH_4^+ \quad 106H_2O \leftrightarrow \text{organics} \quad 16H^+ \quad 106O_2. \qquad [11]$$

Alkalinity sources/sinks from phosphorus uptake and release are an order of magnitude smaller. Note that the alkalinity changes resulting from biological nitrogen uptake are opposite in sign to those generated directly by the original atmospheric deposition flux (Eq. 7). Eventually, most of the extra organic nitrogen will be transported downward and remineralized in subsurface waters, releasing excess NH_4^+ that is almost immediately nitrified to NO_3^- in oxygenated waters.

The net effect of biological nitrogen cycling (case 3) is to reduce surface Δ[Alk] caused by atmospheric nitrogen deposition and to redistribute Δ[Alk] downward through the water column (Fig. 2). The impact, however, does not qualitatively alter the surface water alkalinity perturbations. The strongest negative surface Δ[Alk] anomalies in case 3 are somewhat smaller than those in case 2 but with greater spatial variability and some regions of positive trends (Fig. 3). Some of the spatial variability reflects the patterns of surface nutrient utilization, iron limitation, and the preferential biological uptake of NH_4^+ over NO_3^-. The increase in ocean nitrogen inventory in case 3 is smaller than the cumulative atmospheric nitrogen deposition of 2.7 Tmol·N·y^{-1} because elevated surface NO_3^- and productivity reduces simulated N_2 fixation by 0.6 Tmol·N·y^{-1} and increases denitrification by 0.1 Tmol·N·y^{-1}. Overall, nitrification modulates the acid/base signal from atmospheric nitrogen deposition, and $fAlk_{nitrif}$ with net alkaline effects everywhere is a reasonable approximation for the vertically integrated alkalinity sink in most locations.

Increased primary production stimulated by atmospheric nitrogen deposition lowers surface DIC with a ratio of ≈6.6 C/N (mol/mol) (Eqs. 10 and 11). This results in qualitatively different solutions for pH and air–sea CO_2 flux perturbations (case 3; Fig. 3). The negative Δ[DIC] anomalies are amplified substantially relative to case 2 in some regions, with $\Delta[DIC]/\Delta t$ trends of -0.3 to -0.5 mmol·m^{-3}·y^{-1} over large areas. In many locations, Δ[DIC] decreases faster than Δ[Alk] and thus reverses the sign of the ΔpH signal, with $\Delta pH/\Delta t$ typically ranging from -0.2 to $+0.2 \times 10^{-3}$ pH units·y^{-1}. The case 3 spatial fields are also considerably more patchy, reflecting small-scale readjustments in model primary production, subsurface nutrients, and DIC.

Implications and Future Research

On a global scale, the alterations in surface water chemistry from anthropogenic nitrogen and sulfur deposition are only a few percent of the ocean acidification and Δ[DIC] increases expected from the oceanic uptake of anthropogenic CO_2. However, impacts on seawater chemistry can be much more substantial in coastal waters, on the order of 10–50% or more of the anthropogenic CO_2-driven changes near the major source regions and in marginal seas. Although there are certainly caveats with the simulated coastal signals because the global ocean model does not fully resolve complex coastal physical and biological dynamics, the coastal amplification is clear. Ocean acidification is thought to be a

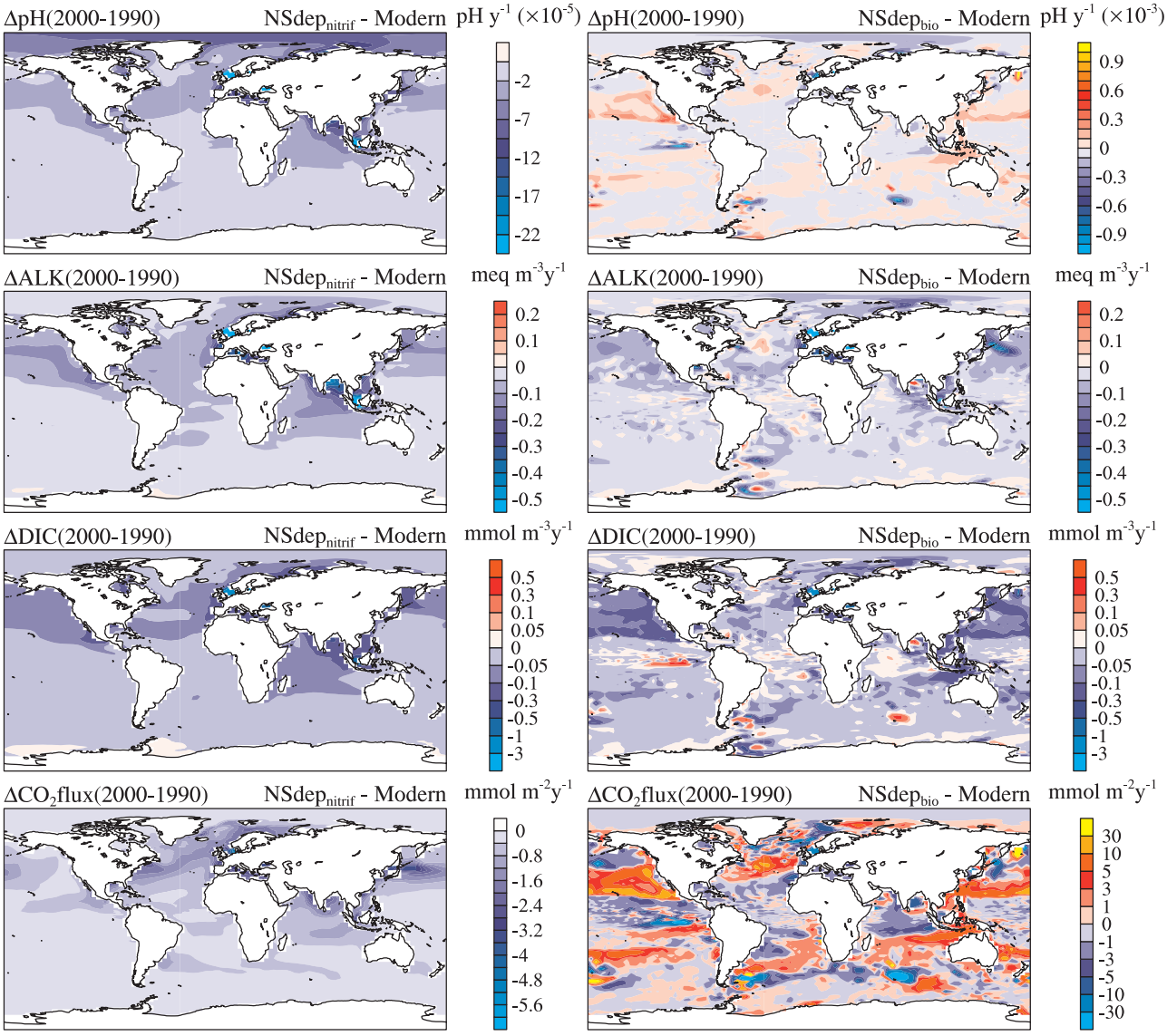

Fig. 3. Perturbation maps of simulated surface water pH, DIC, and total alkalinity trends and air–sea CO_2 flux due to anthropogenic atmospheric nitrogen and sulfur deposition.

significant threat to ecosystems, including coral reefs and coastal benthic and planktonic foodwebs dominated by calcifying organisms (10–13). Our study highlights the need to also consider the effects of non-CO_2 acidification sources from atmospheric nitrogen and sulfur deposition, both through their direct effects on reducing ocean alkalinity and their indirect effects through nitrogen fertilization of marine phytoplankton.

Uncertainties regarding the magnitude of non-CO_2 ocean acidification arise from errors in the anthropogenic sulfur and nitrogen deposition fluxes to the ocean, ocean circulation, and marine biogeochemical responses. Global deposition depends strongly on total emissions, with emission ranges of approximately ±16% for NO_x (total plus lightning) (7, 33), ±27% for NH_x (7, 34), and ±20% for SO_2 (35). Spatial differences in emissions and atmospheric transport pathways will change the downwind deposition fluxes to the oceans. The overall spatial patterns are generally similar across most models but can vary locally because of small shifts in steep deposition gradients. For example, sulfate residence times for models range between 3 and 5 days (35), with our model at 3.4 days. This means that deposition to remote regions in other models could be larger, but that uncertainties should be within ≈50%, even in remote regions. The response of seawater carbonate thermodynamics to acidification is well constrained. Better estimates of the uncertainties due to ocean circulation and biology require exploration of the effect in other numerical models and against field observations.

Here we highlight the first-order impacts associated with anthropogenic atmospheric nitrogen and sulfur. More comprehensive studies on global change and coastal acid/base chemistry would need to include a range of additional processes. The extent of atmospheric neutralization of acidic compounds may be varying because of changes in mineral dust emissions and alkaline fly ash from coal-fired power plants. There is evidence, for example, of reduced atmospheric deposition of basic cations (e.g., Ca^{2+}) (36). Although much of the acidity flux that falls on land will likely be neutralized by soils, some fraction may be transported to the ocean (10, 11, 29), and there are substantial riverine inputs of anthropogenic nitrogen and organic matter to the coastal domain (27, 30, 37). In the water column, second-order biological effects arise from altered rates of nitrogen fixation, water-column and sediment denitrification, calcification, and $CaCO_3$ remineralization (14, 15, 38–40).

Methods

Preindustrial and current nitrogen deposition (including nitrate and ammonia) are simulated (33) in the MOZART model (41), based on climate simulations from the Parallel Climate Model (42) for 1890 and 1990, respectively. Emissions for both preindustrial and present-day come from the EDGAR–HYDE inventory (43). Present-day emissions of ammonia follow ref. 7, whereas preindustrial emissions are assumed to be zero. For the sulfate species, simulations are conducted within the Community Atmospheric Model (CAM3) (44), using sulfate chemistry based on ref. 45. Emissions for preindustrial and current climate for sulfur are based on ref. 46, and the preindustrial and current climates were simulated by using slab ocean model versions (47).

The ocean model combines a state-of-the-art marine ecosystem module (48) with phytoplankton functional groups (pico/nanoplankton, diatoms, diazotrophs, and calcifiers), multiple limiting nutrients (N, P, Si, and Fe), zooplankton, and several detrital pools. The model explicitly tracks both NO_3^- and NH_4^+ pools and includes nitrification, nitrogen fixation, and water-column denitrification (39, 49). The biogeochemistry module (50) has full carbonate system thermodynamics (21), and air–sea CO_2 fluxes follow a quadratic wind-speed gas exchange relationship. The ecobiogeochemistry is embedded in the low-resolution (zonal 3.6°; meridional 0.8°–1.8°; 25 vertical layers with a 12-m-thick surface layer) National Center for Atmospheric Research ocean physical model (CCSM3.1), based on the Parallel Ocean Program (51). This model is integrated with a repeat annual cycle of surface forcing based on National Centers for Environmental Prediction reanalysis and satellite data products (52–54).

This work was supported by National Aeronautics and Space Administration Grant NNG05GG30G and National Science Foundation (NSF) Grant ATM06-28582 (to S.C.D. and I.L.), National Oceanic and Atmospheric Administration Grant GC05-285 (to R.A.F.), and NSF Grants EAR02-23509 and ATM04-39051 (to F.T.M.). The National Center for Atmospheric Research is supported by the NSF.

1. Intergovernmental Panel on Climate Change (2001) *Climate Change 2001: The Scientific Basis*, eds Houghton JT, Ding Y, Griggs DJ, Noguer M, van der Linden PJ, Dai X, Maskell K, Johnson CA (Cambridge Univ Press, New York).
2. Mackenzie FT (1995) in *Biotic Feedbacks in the Global Climatic System*, eds Woodwell G, Mackenzie FT (Oxford Univ Press, New York), pp 22–46.
3. Schlesinger WH (1997) *Biogeochemistry: An Analysis of Global Change* (Academic, San Diego).
4. National Acid Precipitation Assessment Program (1991) *Acidic Deposition: State of Science and Technology*, ed Irving PM (Govt Printing Office, Washington, DC), Vol 1.
5. Howarth RW, Billen G, Swaney D, Townsend A, Jaworski N, Lajtha K, Downing JA, Elmgren R, Caraco N, Jordan T, *et al.* (1996) *Biogeochemistry* 35:75–139.
6. Rodhe H, Dentener F, Schulz M (2002) *Environ Sci Technol* 36:4382–4388.
7. Dentener F, Drevet J, Lamarque JF, Bey I, Eickhout B, Fiore AM, Hauglustaine D, Horowitz LW, Krol M, Kulshrestha UC, *et al.* (2006) *Global Biogeochem Cycles* 20:GB4003.
8. Likens GE, Bormann HF, Johnson NM (1981) in *Some Perspectives of the Major Biogeochemical Cycles*, ed Likens GE (Wiley, New York), SCOPE Report No 17, pp 93–112.
9. Driscoll CT, Lawrence GB, Bulger AJ, Butler TJ, Cronan CS, Eagar C, Lambert KF, Likens GE, Stoddard JL, Weathers KC (2001) *Biosciences* 51:180–198.
10. Galloway JN (2001) *Water Air Soil Pollut* 130:17–24.
11. Galloway JN (2003) in *Interactions of the Major Biogeochemical Cycles*, eds Melillo JM, Field CB, Moldan B (Island Press, Washington, DC), pp 259–272.
12. Orr JC, Fabry VJ, Aumont O, Bopp L, Doney SC, Feely RA, Gnanadesikan A, Gruber N, Ishida A, Joos F, *et al.* (2005) *Nature* 437:681–686.
13. Kleypas JA, Feely RA, Fabry VJ, Langdon C, Sabine CL, Robbins LL (2006) *Impacts of Ocean Acidification on Coral Reefs and Other Marine Calcifiers: A Guide for Future Research* (Univ Corp Atmos Res, Boulder, CO).
14. Feely RA, Sabine CL, Lee K, Berelson W, Kleypas J, Fabry VJ, Millero FJ (2004) *Science* 305:362–366.
15. Andersson AJ, Mackenzie FT, Lerman A (2006) *Global Biogeochem Cycles* 20:GB1S92.
16. Jickells TD (1998) *Science* 281:217–222.
17. Zeebe RE, Wolf-Gladrow D (2005) *CO_2 in Seawater: Equilibrium, Kinetics, Isotopes* (Elsevier, Amsterdam).
18. Sabine CL, Feely RA, Gruber N, Key RM, Lee K, Bullister JL, Wanninkhof R, Wong CS, Wallace DWR, Tilbrook B, *et al.* (2004) *Science* 305:367–371.
19. Dickson AG (1981) *Deep-Sea Res* 28:609–623.
20. Morel FMM (1983) *Principles of Aquatic Chemistry* (Wiley, New York).
21. Department of Energy (1994) *Handbook of Methods for the Analysis of the Various Parameters of the Carbon Dioxide System in Sea Water*, eds Dickson AG, Goyet C (ORNL/CDIAC-74) (Oak Ridge National Laboratory, US Dept Energy, Oak Ridge, TN). Available at http://cdiac.ornl.gov/oceans/handbook.html.
22. Morse JW, Mackenzie FT (2006) *Geochemistry of Sedimentary Carbonates* (Elsevier, Amsterdam).
23. Nakicenovic N, Alcamo J, Davis G, de Vries B, Fenhann J, Gaffin S, Gregory K, Grübler A, Jung TY, Kram T, *et al.* (2000) *Emissions Scenarios: A Special Report of Working Group III of the Intergovernmental Panel on Climate Change* (Cambridge Univ Press, New York).
24. Doney SC (1999) *Global Biogeochem Cycles* 13:705–714.
25. Mikaloff Fletcher SE, Gruber N, Jacobson AR, Doney SC, Dutkiewicz S, Gerber S, Follows M, Joos F, Lindsay K, Menemenlis D, *et al.* (2006) *Global Biogeochem Cycles* 20:GB2002.
26. Ver LM, Mackenzie FT, Lerman A (1999) *Am J Sci* 299:762–801.
27. Mackenzie FT, Ver LM, Lerman A (2002) *Chem Geol* 190:13–32.
28. Paerl HW (1993) *Can J Fish Aquat Sci* 50:2254–2269.
29. Mackenzie FT, Ver LM, Sabine C, Lane M, Lerman A (1993) in *Interactions of C, N, P, and S Biogeochemical Cycles and Global Change*, eds Wollast R, Mackenzie FT, Chou L (Springer, Berlin), pp 1–62.
30. Galloway JN, Dentener FJ, Capone DG, Boyer EW, Howarth RW, Seitzinger SP, Asner GP, Cleveland CC, Green PA, Holland EA, *et al.* (2004) *Biogeochemistry* 70:153–226.
31. Brewer PG, Goldman JC (1976) *Limnol Oceanogr* 21:108–117.
32. Goldman JC, Brewer PG (1980) *Limnol Oceanogr* 25:352–357.
33. Lamarque J-F, Kiehl JT, Brasseur GP, Butler T, Cameron-Smith P, Collins WD, Collins WJ, Granier C, Hauglustaine D, Hess PG, *et al.* (2005) *J Geophys Res* 110:D19303.
34. Bouwman AF, Lee DS, Asman WAH, Dentener FJ, Van Der Hoek KW, Olivier JGJ (1997) *Global Biogeochem Cycles* 11:561–588.
35. Textor C, Schulz M, Guibert S, Kinne S, Balkanski Y, Bauer S, Berntsen T, Berglen T, Boucher O, Chin M, *et al.* (2006) *Atmos Chem Phys* 6:1777–1813.
36. Hedin LO, Granat L, Likens GE, Adri Buishand T, Galloway JN, Butler TJ, Rodhe H (1994) *Nature* 367:351–354.
37. Boyer EW, Howarth RW, Galloway JN, Dentener FJ, Green PA, Vorosmarty CJ (2006) *Global Biogeochem Cycles* 20:GB1S91.
38. Fennel K, Wilkin J, Levin J, Moisan J, O'Reilly J, Haidvogel D (2006) *Global Biogeochem Cycles* 20:GB3007.
39. Moore JK, Doney SC (2007) *Global Biogeochem Cycles* 21:GB2001.
40. Krishnamurthy A, Moore JK, Luo C, Zender CS (2007) *J Geophys Res* 112:G02019.
41. Horowitz LW, Walters S, Mauzerall DL, Emmons LK, Rasch PJ, Granier C, Tie X, Lamarque J-F, Schultz MG, Tyndall GS, *et al.* (2003) *J Geophys Res* 108:4784.
42. Washington WM, Weatherly JW, Meehl GA, Semtner AJ, Jr, Bettge TW, Craig AP, Strand WG, Jr, Arblaster J, Wayland VB, James R, Zhang Y (2000) *Clim Dyn* 16:755–774.
43. van Aardenne JA, Dentener FJ, Olivier JGJ, Klein CGM (2001) *Global Biogeochem Cycles* 15:909–928.
44. Collins WD, Blackmon M, Bitz CM, Bonan GB, Bretherton CS, Carton JA, Chang P, Doney S, Hack JJ, Kiehl JT, *et al.* (2006) *J Clim* 19:2122–2143.
45. Rasch PJ, Collins W, Eaton BE (2001) *J Geophys Res* 106:7337–7355.
46. Smith SJ, Conception E, Andres R, Lurz J (2004) *Historical Sulfur Dioxide Emissions 1850–2000: Methods and Results* (Pacific Northwest Natl Lab, Richland, WA), PNNL-14537.
47. Kiehl J, Shields C, Hack J, Collins W (2006) *J Clim* 19:2584–2596.
48. Moore JK, Doney SC, Lindsay K (2004) *Global Biogeochem Cycles* 18:GB4028.
49. Moore JK, Doney SC, Lindsay K, Mahowald N, Michaels AF (2006) *Tellus B Chem Phys Meteorol* 58:560–572.
50. Doney SC, Lindsay K, Fung I, John J (2006) *J Clim* 19:3033–3054.
51. Smith R, Gent P (2004) *Reference Manual for the Parallel Ocean Program (POP)* (Los Alamos Natl Lab, Los Alamos, NM), LAUR-02-2484.
52. Doney SC, Large WG, Bryan FO (1998) *J Clim* 11:1420–1441.
53. Large WG, Yeager SG (2004) *Diurnal to Decadal Global Forcing for Ocean and Sea-Ice Models: The Data Sets and Flux Climatologies* (Natl Center Atmos Res, Boulder, CO), Technical Note NCAR/TN-460+STR.
54. Doney SC, Yeager S, Danabasoglu G, Large WG, McWilliams JC, *J Phys Oceanogr* 37:1918–1938.